

High-Pressure (1 Torr) Scanning Tunneling Microscopy (STM) Study of the Coadsorption and Exchange of CO and NO on the Rh(111) Crystal Face

Keith B. Rider,[†] Kevin S. Hwang, Miquel Salmeron, and Gabor A. Somorjai*

Contribution from the Department of Chemistry, University of California at Berkeley, and Materials Science Division, Lawrence Berkeley National Laboratory, Berkeley, California 94720

Received January 10, 2002

Abstract: The coadsorption of CO and NO on Rh(111) at room temperature was studied with scanning tunneling microscopy (STM) in the catalytically relevant range of ~ 1 Torr. For gas mixtures where NO is not in large excess, a mixed layer with (2×2) structure is formed. The difference in binding energy between CO and NO on top sites was determined from the measured surface (by direct counting in STM images) and gas mole fractions of each species. A model for the molecular structure is proposed based on the analysis of exchange events between CO and NO molecules in the images. In this model as the partial pressure of NO increases, NO molecules occupy hollow sites first, by displacing CO, and top sites later, where they coexist with CO. As the surface fraction of NO increases, favorable NO–NO interactions cause the formation of segregated NO-rich regions. As with pure NO, a phase transition from the (2×2) -NO to the (3×3) -NO structure takes place in the NO-rich regions at high NO concentration. These results demonstrate the unique ability of STM to obtain molecular-level information under catalytic pressure conditions.

1. Introduction

Scanning tunneling microscopy (STM) provides atomic and molecular resolution images of surface metal atoms and molecules adsorbed on surfaces as long as their motions along the surface are slower than the scanning speed of the tunneling tip, about 100 Å/s. We have constructed an STM instrument that operates at high ambient pressures, up to 1 atm, the first of its kind. The advantage of such a system is that it permits surface studies with the adsorbed species in equilibrium with the gas. Thus, we can obtain adsorption isotherms with molecular scale details of surface structures of adsorbed molecules as the coverage changes as a function of pressure.¹

The interaction between coadsorbed CO and NO on rhodium is of interest due to the reduction of NO by CO in automobile catalytic converters. Modern engines produce exhaust gases with combined CO and NO partial pressures of approximately 5 Torr. Rhodium particles in the catalytic converter are responsible for catalyzing the reaction $\text{CO} + \text{NO} \rightarrow \frac{1}{2}\text{N}_2 + \text{CO}_2$. Nearly all the kinetic models proposed^{2–13} agree (6 and 7 are exceptions) that the initial steps are the adsorption of CO and NO followed

by the dissociation of NO. Although many studies in ultrahigh vacuum (UHV) and in ambient pressures have been performed in an effort to understand this reaction,¹⁴ a detailed molecular understanding of the CO and NO structures and interactions in the Torr pressure range has not previously been acquired.

In this paper we report on investigations of the coadsorption of two molecules, CO and NO, at high pressures, in equilibrium with the gas phase using our high-pressure STM. We detected a mixed molecular surface structure with a (2×2) unit cell below 65% NO coverage. STM can monitor the exchange of CO and NO as the partial pressures of these gases are varied. The difference in CO and NO binding energies at top metal sites has been determined and the surface segregation of NO is monitored as the NO pressure is increased. The observations can be explained by a model in which CO and NO occupy and displace each other at top and hollow sites on the Rh(111) crystal face.

2. Experimental Section

All experiments were carried out in a system consisting of an ultrahigh vacuum chamber containing the surface science analysis and preparation techniques, and a smaller chamber attached to it containing

* Corresponding author. E-mail: somorjai@socrates.berkeley.edu.
[†] Present address: Department of Natural Science, Longwood College, 201 High Street, Farmville, Virginia 23909.
(1) Rider, K. B.; Hwang, K. S.; Salmeron, M.; Somorjai, G. A. *Phys. Rev. Lett.* **2001**, *86*, 4330–4333.
(2) Permana, H.; Ng, K. Y. S.; Peden, C. H. F.; Schmieg, S. J.; Lambert, D. K.; Belton, D. N. *J. Catal.* **1996**, *164*, 194–206.
(3) Campbell, C. T.; White, J. M. *Appl. Surf. Sci.* **1978**, *1*, 347–359.
(4) Dubois, L. H.; Hansma, P. K.; Somorjai, G. A. *J. Catal.* **1980**, *65*, 318–327.
(5) Hecker, W. C.; Bell, A. T. *J. Catal.* **1983**, *84*, 200–215.
(6) Hendershot, R. E.; Hansen, R. S. *J. Catal.* **1986**, *98*, 150–165.
(7) Lintz, H.-G.; Weisker, T. *Appl. Surf. Sci.* **1985**, *24*, 259–267.

(8) Schwartz, S. B.; Fisher, G.; Schmidt, L. D. *J. Phys. Chem.* **1988**, *92*, 389–395.
(9) Peden, C. H. F.; Goodman, D. W.; Blair, D. S.; Berlowitz, P. J.; Fisher, G. B.; Oh, S. H. *J. Phys. Chem.* **1988**, *92*, 1563–1567.
(10) Cho, B. K.; Shanks, B. H.; Bailey, J. E. *J. Catal.* **1989**, *115*, 486–499.
(11) Ng, K. Y. S.; Belton, D. N.; Schmieg, S. J.; Fisher, G. B. *J. Catal.* **1994**, *146*, 394–406.
(12) Peden, C. H. F.; Belton, D. N.; Schmieg, S. J. *J. Catal.* **1995**, *155*, 204–218.
(13) Permana, H.; Ng, K. Y. S.; Peden, C. H. F.; Schmieg, S. J.; Belton, D. N. *J. Phys. Chem.* **1995**, *99*, 16344–16350.
(14) Zhdanov, V. P.; Kasemo, B. *Surf. Sci. Rep.* **1997**, *29*, 35–90.

the STM.^{15,16} The STM, from RHK Technologies, was operated in the 10^{-10} – 10^3 Torr pressure and 300–700 K temperature ranges. The base pressure of the system was 5×10^{-10} Torr, with the background made up primarily of H₂, CO, and water.

The sample was prepared by sputtering with 400 eV oxygen ions for 10 min followed by annealing in a vacuum at 973 K for 2 min. Just before the sample was exposed to CO or NO, it was flashed again briefly to 973 K. The sample temperature was monitored with a chromel–alumel thermocouple mounted in the sample holder in contact with the edge of the crystal, and sample cleanliness was checked with Auger spectroscopy. The clean, room-temperature sample was then transferred to the STM chamber. Large-scale images of the sample showed steps with no preferred orientation, with a spacing that corresponds to a crystal miscut angle less than 1°.

To prevent dissociation of NO, a surface layer of pure CO was prepared by establishing a background pressure of this gas of 10^{-7} Torr over the entire system. Then the gate valve separating the STM chamber from the chamber with the surface science instruments was closed. Because the background pressure was kept while the gate valve was being closed, CO was always the majority species in the gas phase. NO was added later in the STM chamber, after the desired CO pressure had been established. All STM images reported here were acquired with the sample at room temperature.

3. Results

3.1. Mixed (2×2)-3(CO–NO) Structure. Figure 1a shows an STM image of the (2×2) structure formed by CO and NO after addition of 0.15 Torr of NO to the initial 0.50 Torr CO pressure. Although most of the surface is covered with CO (each spot corresponding to a top CO site), new spots 0.3 Å higher than those from the surrounding CO appear (brighter spots). These bright spots represent 1% of the total in this case. Figure 1b shows the surface in a gas mixture consisting of 0.70 Torr of NO and 0.50 Torr of CO. In this case about a quarter of the spots changed contrast from dark to bright. As will be discussed below, the bright spots correspond to top-site NO molecules.

Figure 2 shows a plot of $1/x_{\text{NO},\text{i}}$ vs $1/x_{\text{NO},\text{g}} - 1$, where $x_{\text{NO},\text{i}}$ and $x_{\text{NO},\text{g}}$ are the mole fractions of NO on surface top sites and in the gas phase, respectively. The error bars were calculated from scans averaging 500 molecules each. Due to the finite size of the images it is not surprising that the larger error bars are obtained at the smallest NO coverage. As discussed below the slope of the straight line fit should be $e^{-\Delta E_{\text{i}}/kT}$. The energy ΔE_{i} is the difference between the heats of adsorption of CO and NO on top sites in the coadsorbed layer ($E_{\text{NO},\text{i}} - E_{\text{CO},\text{i}}$). Despite the scattering in the data, the exponential relationship greatly reduces the error in ΔE_{i} , which is found to be -66 ± 5 meV ($=1.5 \pm 0.1$ kcal/mol).

3.2. Site Exchange Processes. When the surface is covered with pure CO or NO, sequential images of the same area appear identical, so that processes such as adsorption, desorption, and diffusion on the surface cannot be observed. When the surface contains both CO and NO, however, top site CO and NO can be distinguished. Inspection of successive images indicates that the surface remains remarkably unchanged except for a few occasional events where a bright spot changes into a dark one and vice-versa, indicating that CO and NO have desorbed, exchanged, or moved. Figure 3 shows a pair of images, each one acquired in 55 s, obtained sequentially on the same area of

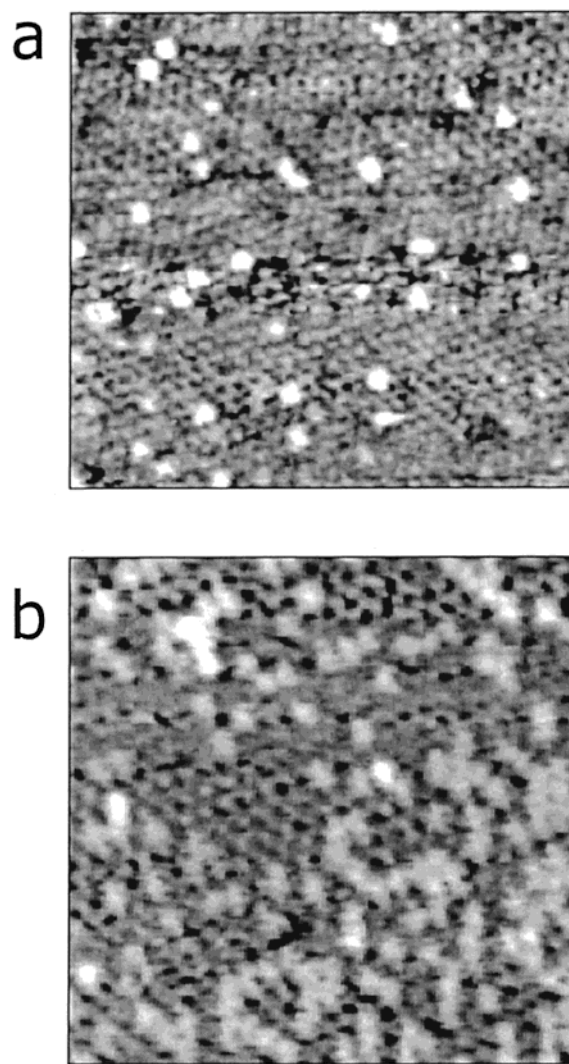


Figure 1. STM images of Rh(111) in equilibrium with a mixture of CO and NO. These $120 \text{ \AA} \times 120 \text{ \AA}$ images display a (2×2) pattern with a corrugation of 0.1 Å, which is characteristic of the (2×2)-3CO structure. The brighter unit cells are due to NO adsorption on the top sites; neither CO nor NO can be seen when it is adsorbed on the hollow-sites. Image a was taken in 0.50 Torr CO + 0.15 Torr NO ($I = 150 \text{ pA}$, $V = 100 \text{ mV}$); image b was taken in 0.50 Torr CO + 0.70 Torr NO ($I = 224 \text{ pA}$, $V = 100 \text{ mV}$). The corrugation of the NO unit cells is 0.5 Å.

the surface. Careful inspection reveals a few displacements and/or substitutions, two of them marked with arrows. After analyzing 10 successive images, each one containing roughly 400 top sites, 64 such events were recorded. This represents a small fraction of the top sites experiencing any change (64 in ~ 4000). The majority of events (56/64) correspond to CO and NO molecules apparently exchanging place with neighboring top sites. A much smaller fraction (5/64) corresponded to a molecule moving two unit cells away, and just 3/64 events resulted in the appearance or disappearance of a top-site NO molecule.

3.3. NO Segregation and Phase Transformation. Another interesting observation is that the spatial distribution of NO molecules is not random, particularly when the top-site occupation is near 50% NO. As the images in Figure 3 show, there is a preference for NO molecules to have other NO molecules in neighboring top sites, with a tendency to form chains along the substrate close packed directions.

(15) Jensen, J. A.; Rider, K. B.; Chen, Y.; Salmeron, M.; Somorjai, G. A. *J. Vac. Sci. Technol. B* **1999**, *17*, 1080–1084.

(16) McIntyre, B. J.; Salmeron, M.; Somorjai, G. A. *Rev. Sci. Instrum.* **1993**, *64*, 687–691.

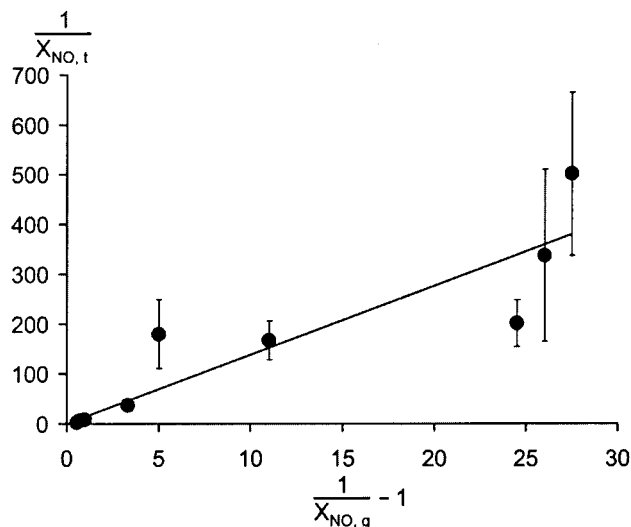


Figure 2. Plot of top-site NO coverage and NO partial pressure. $1/x_{\text{NO},t}$ was plotted vs $(1/x_{\text{NO},g} - 1)$, where $x_{\text{NO},t}$ is the mole fraction of NO on top sites (obtained from the images), and $x_{\text{NO},g}$ is the mole fraction of NO in the gas phase. The slope of the least-squares fit line is $e^{-\Delta E_t/RT}$, where ΔE_t is the difference in adsorption energy between CO and NO on the top site. We calculate this difference to be -66 ± 5 meV. The negative sign indicates that CO binds more strongly to the top site than NO.

When the NO partial pressure is two to four times greater than the CO partial pressure, segregation of areas that are rich in NO takes place producing bright and dark regions in the STM images. The bright regions are dominated by NO and often have elongated shapes as shown in the two images of Figure 4. At sufficiently high NO pressure, eventually (3×3) areas develop inside the bright NO-rich regions. The image in Figure 5 shows an example of a (3×3) region (enclosed by the white broken line) formed in the mixed CO–NO layer in equilibrium with 0.10 Torr of CO and 0.32 Torr of NO. As in the case of pure NO, the contrast in the (3×3) cells is even higher than that in the NO (2×2) cells.

The order of introduction of gases does not affect the final state of the surface. By alternately increasing the NO partial pressure and then the CO partial pressure, the surface structure can be changed from (2×2) to (3×3) and vice versa several times.

4. Discussion

4.1. Mixed (2×2) - $3(\text{CO}-\text{NO})$ Structure. Carbon monoxide adsorbs molecularly^{17–23} forming many different structures.^{17,24–27} The densest layer has a (2×2) - 3CO structure with a unit cell containing one CO molecule in a top site and two molecules in 3-fold hollow sites.^{21–23,28,29} At 300 K this structure forms above

- (17) Peterlinz, K. A.; Curtiss, T. J.; Sibener, S. J. *J. Chem. Phys.* **1991**, *95*, 6972–6985.
 (18) Koestner, R. J.; Van Hove, M. A.; Somorjai, G. A. *Surf. Sci.* **1981**, *107*, 439–458.
 (19) Castner, D. G.; Sexton, B. A.; Somorjai, G. A. *Surf. Sci.* **1978**, *71*, 519–540.
 (20) Thiel, P. A.; Williams, E. D.; Yates, J. T. *Surf. Sci.* **1979**, *84*, 54–64.
 (21) Beutler, A.; Lundgren, E.; Nyholm, R.; Andersen, J. N.; Setlik, B.; Heskett, D. *Surf. Sci.* **1997**, *371*, 381–389.
 (22) Beutler, A.; Lundgren, E.; Nyholm, R.; Andersen, J. N.; Setlik, B.; Heskett, D. *Surf. Sci.* **1998**, *396*, 117–136.
 (23) Gierer, M.; Barbieri, A.; Van Hove, M. A.; Somorjai, G. A. *Surf. Sci.* **1997**, *391*, 176–182.
 (24) Wei, D. H.; Skelton, D. C.; Kevan, S. D. *Surf. Sci.* **1997**, *381*, 49–64.
 (25) Payne, S. H.; Jun, Z.; Kreuzer, H. J. *Surf. Sci.* **1992**, *264*, 185–196.
 (26) Payne, S. H.; Kreuzer, H. J.; Peterlinz, K. A.; Curtiss, T. J.; Uebing, C.; Sibener, S. J. *Surf. Sci.* **1992**, *272*, 102–110.
 (27) Peterson, L. D.; Kevan, S. D. *J. Chem. Phys.* **1991**, *94*, 2281–2293.

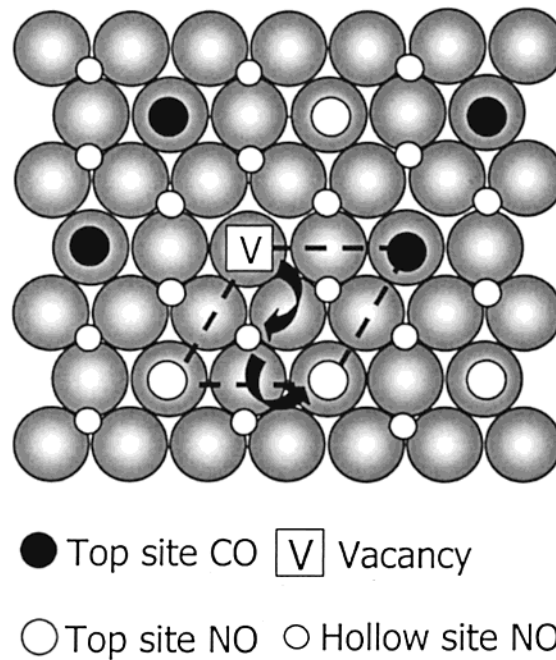
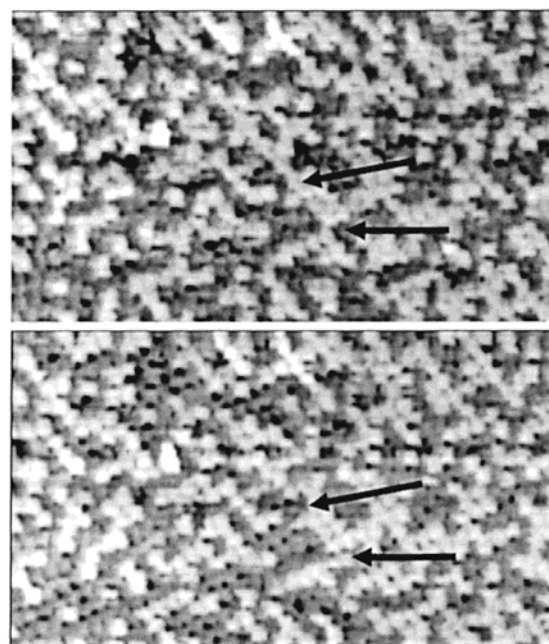


Figure 3. Pair of sequential STM images taken 55 s apart. These $200 \text{ \AA} \times 115 \text{ \AA}$ images were taken on the same area of the surface in 0.50 Torr CO + 0.92 Torr NO ($I = 260$ pA, $V = 50$ mV). The top arrow shows one top site occupied by NO in the top image and by CO in the bottom one. The bottom arrow shows the opposite. The diagram shows how a vacancy (boxed V) can diffuse across the unit cell and be substituted by a neighboring NO molecule, which is found in most of the hollow sites.

10^{-6} Torr and persists until the CO pressure is at least 700 Torr.³⁰ Two peaks, at 510 and 430 K, were observed by temperature-programmed desorption (TPD), an indication that indeed two adsorption sites exist with different binding energy. The adsorption of NO is more complex because it dissociates

- (28) Van Hove, M. A.; Koestner, R. J.; Somorjai, G. A. *Phys. Rev. Lett.* **1983**, *50*, 903–906.
 (29) Van Hove, M. A.; Koestner, R. J.; Frost, J. C.; Somorjai, G. A. *Surf. Sci.* **1983**, *129*, 482–506.
 (30) Cemota, P.; Rider, K.; Yoon, H. A.; Salmeron, M.; Somorjai, G. *Surf. Sci.* **2000**, *445*, 249–255.

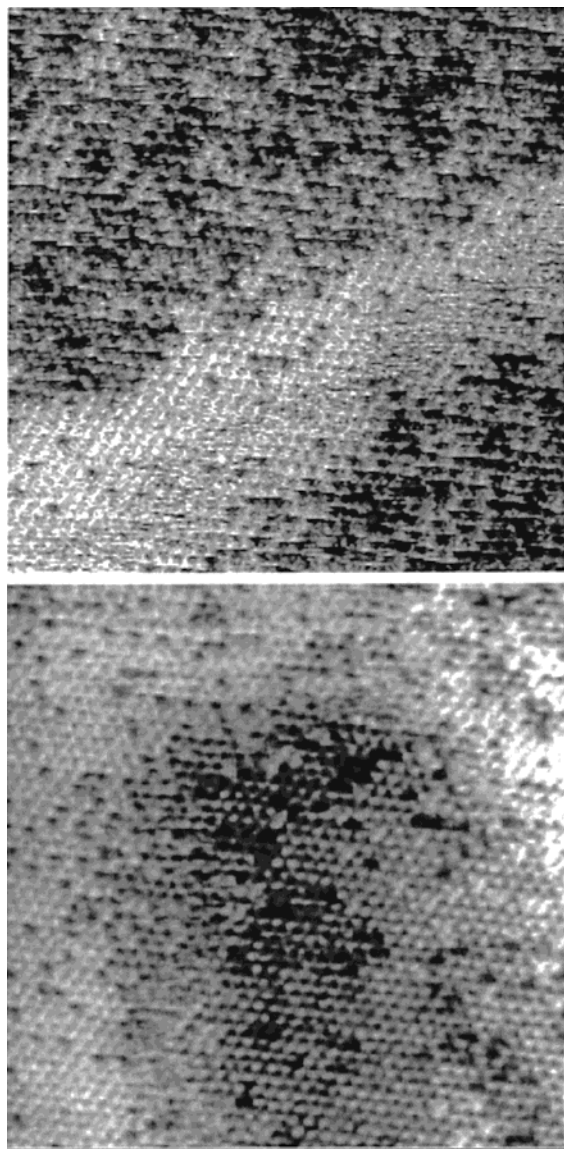


Figure 4. STM images showing formation of NO-rich regions. These $200 \text{ \AA} \times 200 \text{ \AA}$ images were taken in 0.10 Torr CO + 0.32 NO ($I = 177 \text{ mV}$, $V = 100 \text{ mV}$). The (2×2) structure is visible with the top sites being covered with a mixture of CO and NO. The brighter regions have a higher concentration of NO on the top sites.

when the temperature is above 200 K and the coverage is below $1/3 \text{ ML}$.^{19,31–33} Low-energy electron diffraction (LEED)^{34,35} and X-ray photoelectron diffraction (XPD)³⁶ studies have shown that at high coverage (0.75 ML) NO forms a (2×2) -3NO structure analogous to the one formed by CO. An important characteristic of the STM images of the dense (2×2) structures is that only top-site molecules produce a high contrast, while those bound to hollow sites have electronic structures and orbital symmetries that makes their contribution to the tunneling current much

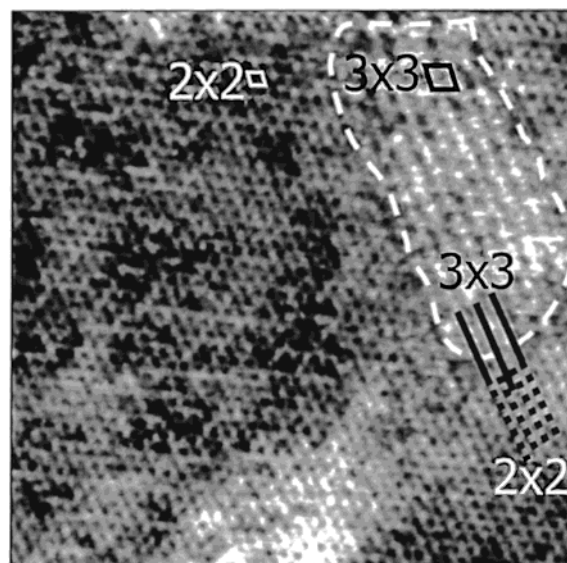


Figure 5. STM image showing formation of the (3×3) structure. The $200 \text{ \AA} \times 200 \text{ \AA}$ image was taken in 0.10 Torr CO + 0.32 Torr NO ($I = 190 \text{ pA}$, $V = 100 \text{ mV}$). The brighter, nearly pure NO regions of the surface are the nucleation sites for the formation of the (3×3) structure that is characteristic of high-pressure NO adsorption. In the absence of CO, the (2×2) to (3×3) phase transition occurs when the pressure rises above 0.03 Torr.

smaller than those on top sites. Thus these molecules are not imaged.³⁷

Electron energy loss spectroscopy (EELS) and TPD experiments have shown that NO and CO have significantly different binding energies on the top and hollow sites.^{31,38} In pure NO layers the molecule binds more strongly to hollow sites at both low and high coverage. In pure CO layers, however, the molecule binds more strongly to top sites at low coverage up to 0.3 monolayers (ML) but switches to hollow sites between 0.3 and 0.5 ML. At higher coverage, the top sites start to populate again.³⁰ When both molecules compete for sites, IR spectroscopy seems to indicate that under catalytic reaction conditions NO binds to hollow sites while CO binds to top sites.^{2,14}

Except when the NO partial pressure is very high, the surface shows a (2×2) structure formed by a mixture of molecules, as shown in Figures 1, 3, and 4. Since the number of bright spots is observed to increase with each increase in the NO partial pressure, we conclude that they correspond to the NO molecules. Unfortunately only the top site molecules are visible in the STM images, so no direct information on the other two molecules in the 3-fold hollow sites of the unit cell is available.

While we have not performed variable-temperature experiments on this system, a previous STM study of pure NO on Rh(111) indicates that the surface is in equilibrium with the gas phase under the experimental conditions.¹ This was demonstrated by the observed phase transition between the (2×2) and (3×3) -NO structures, which occurred at the same temperature after both heating and cooling.

If the exchange of molecules between surface and gas-phase molecules takes place primarily from top sites, which bind the molecules more weakly than the hollow sites, and if we assume

(31) Root, T. W.; Fisher, G. B.; Schmidt, L. D. *J. Chem. Phys.* **1986**, *85*, 4679–4686.

(32) Root, T. W.; Schmidt, L. D.; Fisher, G. B. *Surf. Sci.* **1983**, *134*, 30–45.

(33) Borg, H. J.; Reijerse, J. F. C.-J. M.; van Santen, R. A.; Niemantsverdriet, J. W. *J. Chem. Phys.* **1994**, *101*, 10052–10063.

(34) Kao, C.-T.; Blackman, G. S.; Van Hove, M. A.; Somorjai, G. A.; Chan, C.-M. *Surf. Sci.* **1989**, *224*, 77–96.

(35) Zasada, I.; Van Hove, M. A.; Somorjai, G. A. *Surf. Sci.* **1998**, *418*, L89–L93.

(36) Kim, Y. J.; Thevuthasan, S.; Herman, G. S.; Peden, C. H. F.; Chambers, S. A.; Belton, D. N.; Permana, H. *Surf. Sci.* **1996**, *359*, 269–279.

(37) Sautet, P.; Rose, M. K.; Dunphy, J. C.; Behler, S.; Salmeron, M. *Surf. Sci.* **2000**, *453*, 25–31.

(38) Root, T. W.; Schmidt, L. D.; Fisher, G. B. *Surf. Sci.* **1985**, *150*, 173–192.

that the binding energies on the top sites do not depend on the nature (CO or NO) of the surrounding molecules, then the gas and top site mole fractions of CO and NO should be related by:³⁹

$$\frac{x_{\text{CO,t}}}{x_{\text{NO,t}}} = \frac{x_{\text{CO,g}}}{x_{\text{NO,g}}} e^{-\Delta E_t/kT} \quad (1)$$

where $x_{\text{CO,t}}$, $x_{\text{NO,t}}$ and $x_{\text{CO,g}}$, $x_{\text{NO,g}}$ are the mole fractions of CO and NO on surface top sites and in the gas phase, respectively. Later on we will discuss and justify these assumptions in more detail. The value of ΔE_t was found from the plot in Figure 2 to be -66 ± 5 meV, with the negative sign indicating that CO binds more strongly than NO on the top sites on the saturated surface. Despite the large error in the values of the relative NO and CO top-site coverage, a relatively small value for error in the binding energy difference is obtained. This is due to the logarithmic dependence of ΔE_t on the mole fractions. One should keep in mind the limiting assumptions involved in (1), where interactions between neighboring top-site NO molecules were neglected. We know, however, that this interaction is important at high NO coverage and that it gives rise to the linear clustering and later segregation of NO-rich regions. For that reason the value of ΔE_t should be used with caution at high NO coverage, where (1) will predict values of $x_{\text{NO,t}}$ smaller than those found in the images.

Theoretical studies of low coverage and of isolated molecules predict that NO binds more strongly than CO on top sites.^{40,41} However, no calculations have been performed for the binding energy of the top sites in dense layers that could be compared with the present results.

4.2. Site Exchange Processes. The low frequency of events indicative of any molecular change in the images is at first remarkable. It indicates that despite the high collision rate of gas molecules per site ($\sim 10^6$ s⁻¹ at 1 Torr), most of the impinging molecules are reflected back into the gas phase. It also shows a nearly complete immobility of the molecules, which can be attributed to the dense packing, which blocks diffusion, and the near absence of vacancies. More quantitatively, the probability of a change was measured to be 64/4000 per site over a period of about 600 s during acquisition of the 10 consecutive images. It indicates that molecular desorption events occur at a frequency of $\nu = 2.7 \times 10^{-5}$ s⁻¹. Using the Arrhenius form $\nu = 10^{12} \times e^{-E_t/kT}$ s⁻¹, we can estimate a binding energy E_t of 1.0 eV (=23 kcal/mol) assuming a preexponential factor of 10^{12} s⁻¹ (the value of E_t would change by only 6% per order of magnitude change in the preexponential).

The value of 1 eV is smaller than the calculated values for top site adsorption in the low coverage ($\sqrt{3} \times \sqrt{3}$) structure of 1.68 and 1.90 eV for NO by van Santen et al.⁴⁰ and Sautet et al.⁴¹ respectively, or of 1.46 eV for CO.⁴⁰ Our lower estimated value is not surprising, however, because in the dense (2×2)-3(CO-NO) structure the top sites must feel the repulsion of the neighboring hollow site molecules. Because CO binds 66 meV stronger than NO, its rate of desorption should be approximately 13 times lower. As we discuss below, however,

the visible events in the images are likely to be initiated by CO rather than NO desorption. The value of 1 eV estimated above could be better compared with the value we extrapolated from the CO TPD data of Root et al.,³⁸ who studied the coadsorption of CO and NO. After NO exposure to the CO-covered surface, these authors found a shoulder at 370 K for CO desorption. This temperature implies a binding energy of 1.0 eV, which agrees with our estimate based on the observed frequency of changes (again with the same uncertainty in the preexponential values).

These observations could be explained with the following model. We assume that when NO is introduced, it substitutes for CO primarily in the hollow sites. This is why the images in Figure 1 show only a few bright NO spots, because only top-site NO is visible. This assumption agrees with the TPD results of Root et al.³⁸ These authors observed that after exposing NO to the CO-saturated surface, CO desorbs almost exclusively in a TPD peak at the same temperature as the shoulder in the TPD of the (2×2) structure of pure CO, which is attributed to the top sites. NO desorbs later, after the CO has already completely desorbed.

From then on, with the population of hollow sites comprised largely of NO, the equilibrium with the gas phase is maintained by adsorption/desorption of CO and NO in top sites and lends justification a posteriori to the use of eq 1 above. Once a vacancy is produced by a desorption event, it can be filled either directly from the gas phase or by diffusion of an NO molecule from a neighboring hollow site (see diagram in Figure 3). Unless kinetic barriers to adsorption are assumed, direct filling at this point from the gas phase should lead to a nearly 50% chance that an original top-site NO (which should desorb 13 times more frequently than CO) would be replaced by a CO for a gas composed of 50% NO, thus yielding a net loss of one bright site. Similarly, a desorbing top-site CO immediately filled by a gas phase molecule has about a 50% chance of leading to a net gain of a bright spot. Clearly this is not what is observed, since this would imply many instances of independent gains or losses instead of just exchanges.

It appears then that vacancy diffusion to a neighboring hollow site is more likely. A desorbing top-site CO could then be filled by an adjacent hollow-site NO, changing its appearance in the STM images from dark to bright; if the desorbing molecule was NO instead, refilling by an adjacent hollow site NO molecule would not change top-site contrast and the event would not be observable by STM. The hollow-site vacancy will probably continue to diffuse to a top site occupied by NO since its binding energy is lower (by 66 meV) and finally be refilled from the gas phase. This top site is probably very close to the original, since at room temperature its lifetime should be very short. Restoration of the equilibrium fractional coverages demands that, in the average, a CO molecule from the gas phase should fill the vacancy. The details of the mechanisms involved are not presently understood, though they probably must include the energetics of the interactions between neighboring CO and NO molecules and their dependence on site geometry. Better statistics and more experimental data are necessary to fully understand this.

4.3. NO Segregation and Phase Transformation. The alignment of top-site NO molecules observed in Figure 3 suggests that second nearest neighbor (top-site/top-site) NO-

(39) It is also assumed that the preexponential factors for CO and NO desorption are the same.

(40) Koper, M. T. M.; van Santen, R. A.; Wasileski, S. A.; Weaver, M. J. *J. Chem. Phys.* **2000**, *113*, 4392-4407.

(41) Loffreda, D.; Simon, D.; Sautet, P. *Chem. Phys. Lett.* **1998**, *291*, 15-23.

NO interactions are more favorable than NO–CO interactions. This implies also that the difference between the NO–NO and NO–CO second nearest interactions is of the order of kT , 25 meV ($=kT$ at room temperature). For comparison, at low coverage ($\theta = 1/3$), Payne et al.²⁶ reported a CO–CO attraction of 7 meV. At higher partial pressures of NO, where images show light and dark areas as in Figure 4, the degree of brightness is probably correlated with the concentration of NO.

In previous work, we reported that pure NO forms a (2×2) -3NO structure in equilibrium with the gas phase up to 0.03 Torr and then undergoes a phase transition to a (3×3) -7NO structure.¹ In this new structure, the top NO is again the only molecule imaged by the STM in the unit cell. In addition, it shows higher contrast than that of the top site in the (2×2) -3NO structure. The presence of CO considerably alters the equilibrium NO pressure required for this transition, which now occurs at a much higher NO partial pressure. When this pressure is high enough, however, (3×3) areas develop inside the bright regions, as shown in Figure 5. As indicated above, in order for the (3×3) structure to form the NO partial pressure must be three to five times greater than the CO partial pressure at room temperature. For 0.1 Torr of CO, for example, this is 10 times larger than that required with pure NO.

5. Conclusions

We have studied the molecular structure of the surface layer formed on Rh(111) in equilibrium with NO–CO gas mixtures at partial pressures in the regime relevant to automobile catalytic converters. At low NO partial pressures, the molecules mix into a (2×2) -3(CO–NO) structure. In the dense (2×2) structures formed at high pressure, neither CO nor NO is visible in the

STM images when adsorbed on hollow sites. They do appear as distinct spots when on top sites with an apparent height difference of 0.3 Å in favor of NO. From the equilibrium concentration of top-site molecules, we find that top-site CO is more stable than top-site NO by 66 ± 5 meV.

On the basis of the low rate of changes and the NO pressure necessary to produce bright NO spots in the images, we have proposed a model where NO substitutes for CO in the hollow sites first and then on the top sites later. Molecular desorption from the top sites occurs at frequencies of the order of 10^{-5} s⁻¹, which implies an adsorption energy of 1.0 eV. The occasional exchange of contrast observed in the STM images between neighboring CO and NO top sites is explained by a vacancy-mediated diffusion mechanism, though the details are not presently understood.

There appears to be a slight preference for NO molecules to occupy adjacent top sites in the (2×2) lattice, which causes the formation of NO-rich islands at higher NO partial pressures. The presence of CO in the gas phase increases the NO partial pressure that is necessary for the formation of the NO (3×3) structure until the NO partial pressure is three to five times greater than the CO partial pressure. When the (3×3) structure forms, it nucleates on the NO-rich areas mentioned above.

Acknowledgment. This work was supported by the Director, Office of Science, Office of Basic Energy Sciences, Division of Materials Sciences and Engineering, of the U.S. Department of Energy under Contract No. DE-AC03-76SF00098. One of us (K.S.H.) is grateful to the Chevron Corporation for a graduate student fellowship.

JA020055W